The current issue and full text archive of this journal is available at
www.emeraldinsight.com/0264-4401.htm

Received 6 February 2007
Revised 12 February 2008
Accepted 14 February 2008

Natural sloshing frequencies in rigid truncated conical tanks

I. Gavrilyuk
Staatliche Studienakademie Thüringen- Berufsakademie Eisenach, University of Cooperative Education, Eisenach, Germany

M. Hermann
Friedrich-Schiller-Universität Jena, Jena, Germany

I. Lukovsky and O. Solodun
Institute of Mathematics, National Academy of Sciences of Ukraine, Kiev, Ukraine, and

A. Timokha
Centre of Excellence "Centre for Ship and Ocean Structures", Norwegian University of Science and Technology, Trondheim, Norway

Abstract

Purpose – The main purpose of this paper is to develop two efficient and accurate numerical analytical methods for engineering computation of natural sloshing frequencies and modes i the case of truncated circular conical tanks.

Design/methodology/approach – The numerical-analytical methods are based on a Ritz Treftz variational scheme with two distinct analytical harmonic functional bases.

Findings – Comparative numerical analysis detects the limit of applicability of variational methods in terms of the semi-apex angle and the ratio between radii of the mean free surface and the circular bottom. The limits are caused by different analytical properties of the employed functional bases. However, parallel use of two or more bases makes it possible to give an accurate approximation of the lower natural frequencies for relevant tanks. For V-shaped tanks, dependencies of the lowest natural frequency versus the semi-apex angle and the liquid depth are described.

Practical implications – The methods provide the natural sloshing frequencies for V-shaped tanks that are valuable for designing elevated containers in seismic areas. Approximate natural modes can be used in derivations of nonlinear modal systems, which describe a resonant coupling with structural vibrations.

Originality/value – Although variational methods have been widely used for computing the natural sloshing frequencies, this paper presents their application for truncated conical tanks for the first time. An original point is the use of two distinct functional bases.

Keywords Numerical analysis, Frequencies, Liquid flow containers

Paper type Research paper

1. Introduction

The number of constructions carrying a large liquid mass is enormous. Coupling the structure and liquid requires a precise and efficient computation of the natural sloshing

The authors thank the German Research Society (DFG) for financial support (project DFG 436UKR 113/33/00). The last author is grateful for the sponsorship of the Alexander von Humboldt Foundation.

Engineering Computations: International Journal for Computer-Aided Engineering and Software
Vol. 25 No. 6, 2008
pp. 518-540

0264-4401
DOI 10.1108/02644400810891535

(eigen-) frequencies and modes. Being subject of spacecraft applications, the natural sloshing frequencies and modes for conical tanks were studied in 1950-1960's years of the past century. Special attention was paid to an estimate of the resulting hydrodynamic force and moment.

The international standards concerning the megaliter elevated tanks (Eurocode 8, 1998) have stated a typical design for concrete tanks of conical and conicalbottom shapes, typical examples are demonstrated by Damatty and Sweedan (2006). Owing to seismic events, liquid motions in a water tank on the supporting tower cause severe hydrodynamical loads. In the modelling of these loads, equivalent mechanical systems (Damatty and Sweedan, 2006; Dutta *et al.*, 2004; Shrimali and Jangid, 2003) can be used. These systems relate liquid dynamics to oscillations of a pendulum or a spring-mass system. The eigenfrequencies of the equivalent systems should coincide with the lower natural sloshing frequencies and, therefore, an accurate prediction of the sloshing frequencies and modes is needed (Damatty *et al.*, 2000; Dutta and Laha, 2000; Tang, 1999). This can be done by various Computational Fluid Dynamics (CFD) methods or by using semi-empirical approximate formulae (Damatty *et al.*, 2000; Gavrilyuk *et al.*, 2005). Although the CFD-methods demand lots of CPU's power, they are primary employed in engineering practise to guarantee a substantial precision. When concentrating on linear and nonlinear sloshing in V-shaped pure conical tanks, Gavrilyuk *et al.* (2005) showed that an alternative might consist in a semianalytical solution method. The method keeps the accuracy of the CFD-methods, but remains CPU-efficient and simple in use. The constructed numerical-analytical solutions may facilitate development of nonlinear sloshing theories (Lukovsky and Bilyk, 1985; Lukovsky, 1990, 2004; Bauer and Eidel, 1988; Faltinsen *et al.*, 2000, 2003; Gavrilyuk *et al.*, 2005, 2006). These theories are of importance for studying a resonant coupled vibration of a tower and the contained liquid.

In order to find the natural sloshing frequencies and modes, a spectral boundary value problem (Lukovsky *et al.*, 1984; Ibrahim, 2005) has to be solved. When the tank is V- and Λ- shaped, the boundary value problem has no analytical solutions. Isolated analytical solutions exist only for pure (non-truncated) conical V-tanks. Such an example has been specified by Levin (1963) for the two lowest natural modes and the semiapex angle $\theta_0 = 45°$. These modes are characterised by the wave number $m = 1$ in angular direction. Dokuchaev and Lukovsky (1968) generalised this result. They showed that analogous analytical solutions exist as $\theta_0 = \arctan(\sqrt{m})$. Mikishev and Rabinovich (1968) and Feschenko *et al.* (1969) used these solutions for evaluation of their numerical algorithms. Furthermore, simple approximate analytical solutions for pure conical V-tanks can be obtained by replacing the planar waterplane by a spheric segment. In that case, the spectral boundary value problem admits separation of variables in the spherical coordinate system. This has been realised by Dokuchaev (1964) and Bauer (1982). A satisfactory agreement with experimental data by Mikishev and Dorozhkin (1961) and Bauer (1982) was reported as $\theta_0 = 15°$.

The spectral boundary value problem for the linear sloshing modes admits a variational formulation (Feschenko *et al.*, 1969). This variational formulation facilitates the Ritz-Treftz numerical scheme, whose practical realisation requires special sets of analytical harmonic functional bases. Two of these harmonic bases are used in the present paper for engineering computations of the natural frequencies and modes of liquid sloshing in truncated conical tanks. The first basis is of polynomial type (harmonic polynomial solutions, HPS). The second one employs the Legendre functions of first kind; it may be adopted by the mentioned nonlinear multimodal sloshing theories. Extensive numerical experiments have been done to identify all the geometrical parameters (semi-apex angle, position of secant plane and liquid depth), for which the proposed functional bases guarantee a sufficient number of significant figures for the lower natural frequencies.

In Section 3, the main focus is on the HPS. For the V-shaped tanks, we show that 11-17 HPS provide 4-6 significant digits of the lower natural frequencies for the semi-apex angles, which are smaller than 75° and larger than 10°. For the V- and Λ-shaped tanks which are characterised by semi-apex angles larger than 75°, the same number of the HPS guarantees 3-4 significant digits. For the Λ-shaped tanks with semi-apex angles smaller than 75°, convergence to the natural frequencies depends on the ratio between the radii of the mean liquid plane and the circular bottom. The method is not very efficient (only about 2-3 significant digits can be obtained with 17-20 basic polynomials) when the semi-apex angle is smaller than 60° and the ratio between the specified radii is smaller than 1/2. The slow convergence for the Λ-shaped tanks can partially be attributed to a singular asymptotic behaviour of the natural modes at the contact line formed by the waterplane and conical walls.

Lukovsky (1990) has proposed a non-conformal mapping technique to develop the multimodal method for the nonlinear sloshing problem in a non-cylindrical tank. Lukovsky and Timokha (2002) and Gavrilyuk *et al.* (2005) have realised this technique for a non-truncated V-tank. The natural sloshing modes were then approximated by a special functional basis (SFB). In Section 4, we use the curvilinear coordinate system proposed by Gavrilyuk *et al.* (2005) and generalise their results on natural sloshing frequencies to the case of truncated V- and Λ-shaped conical tanks. For typical geometrical configurations of elevated water tanks (a V-shaped cone with the semi-apex angle between 30° and 60°), the method shows faster convergence behaviour than in the case of Section 3. Six significant digits of the lowest sloshing frequency can be computed by using only 6-10 basis functions.

A comparative analysis of the two methods is presented in Section 5. In Section 6, we discuss the dependence of the lowest natural sloshing frequency on the geometrical shape of truncated conical tanks. Bearing in mind that the relevant water tanks are of a V-shape, we present the lowest spectral parameter (with a accuracy of five significant digits) versus the semi-apex angle and the ratio between the radii of the mean water plane and the bottom.

2. Statement of the problem

2.1 Differential and variational formulations

As it is typically assumed in sloshing theory (Ibrahim, 2005), we consider an ideal incompressible liquid with irrotational flow that partly occupies an earth-fixed rigid conical tank with the semi apex angle θ_0. The mean (hydrostatic) liquid shape coincides with the domain Q_0 as it is shown in Figure 1. The gravity acceleration is directed downwards along the symmetry axis Ox. The wetted conical walls are denoted by S_1. The circle S_2 is the tank bottom, $S = S_1 \cup S_2$ and $\sum_0$ is the non-perturbed (hydrostatic) waterplane. The origin is superposed with artificial apex of the conical surface. Henceforth, the problem is considered in a sizeless statement assuming that r_0 (the bottom radius for Λ-shaped and the water plane radius for V-shaped tanks)

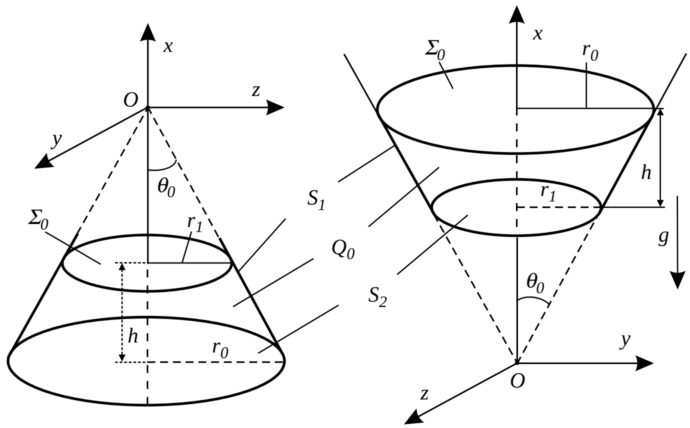

Figure 1.
Hydrostatic liquid domains in Λ- and V-haped tanks

is chosen as a characteristic geometrical dimension. Scaling by r_0 implies $h := h/r_0 \to 0$ (h is the liquid depth) and $r_1 := r_1/r_0$. The non-dimensional radius r_1 and the angle θ_0 completely determine the geometric proportions of Q_0. The limit $r_1 \to 1$ implies that $h \to 0$, ie. the water becomes shallow. At a fixed r_1, the scaled liquid depth h tends to zero as $\theta_0 \to \pi/2$.

Linear sloshing in a motionless tank is governed by the following boundary value problem (Lukovsky *et al.*, 1984; Ibrahim, 2005):

$$\Delta\phi = 0 \,\text{in}\, Q_0; \quad \frac{\partial\phi}{\partial x} = \frac{\partial f}{\partial t}, \quad \frac{\partial\phi}{\partial t} + gf = 0 \,\text{on} \sum\nolimits_0; \quad \frac{\partial\phi}{\partial n} = 0 \,\text{on}\, S; \quad \int_{\sum_0} \frac{\partial\phi}{\partial x}\mathrm{d}S = 0, \tag{1}$$

where $\phi(x,y,z,t)$ is the velocity potential, $x = f(y,z,t)$ describes the free surface, n is the outer normal to S and g is the gravity acceleration scaled by $r_0(g := g/r_0)$. The initial conditions:

$$f(y,z,t_0) = F_0(y,z); \quad \frac{\partial f}{\partial t}(y,z,t_0) = F_1(y,z) \tag{2}$$

at an instant time $t = t_0$, determine a unique solution of equation (1). The functions F_0 and F_1 define initial displacements of the free surface and its velocity, respectively.

2.2 Natural sloshing modes

The solution of equation (1) is associated with the free-standing waves:

$$\phi(x,y,z,t) = \psi(x,y,z)\exp(i\sigma t), \quad i^2 = -1 \tag{3}$$

where a is the natural sloshing frequency and $\psi(x,y,z)$ is the so-called natural mode. Inserting equation (3) into equation (1) leads to the spectral problem:

$$\Delta\psi = 0 \,\text{in}\, Q_0; \quad \frac{\partial\psi}{\partial x} = \kappa\psi \,\text{on} \sum\nolimits_0; \quad \frac{\partial\psi}{\partial n} = 0 \,\text{on}\, S; \quad \int_{\sum_0} \frac{\partial\psi}{\partial x}\mathrm{d}S = 0 \tag{4}$$

where the eigenvalue κ is defined by:

$$\kappa = \frac{\sigma^2}{g}. \tag{5}$$

The spectral problem (4) has a real positive point wise spectrum (Morand and Ohayon, 1995):

$$0 < \kappa_1 \leq \kappa_2 \leq \ldots \leq \kappa_n \leq \ldots$$

with a unique limit point at infinity, i.e. $\kappa_n \rightarrow \infty, n \rightarrow \infty$. Together with the constant function, projections of the eigenfunctions, $f_n(y,z) = \psi_n|\sum_0$ constitute an orthogonal basis in the mean-squares metrics. Because the velocity potential ϕ satisfies the volume conservation condition (see, the last integral equality in equation (1)), getting known $\{\kappa_n\}$ and $\{\psi_n\}$, one can represent the solution of equation (1) and equation (2) as a Fourier series by $\phi_n = \psi_n(x,y,z)\exp(i\sigma_n t)$, namely, as a superposition of the free-standing waves.

2.3 On the Ritz-Treftz schem for the spectral problem (4)

Problem (4) admits a minimax variational formulation (Feschenko *et al.*, 1969; Morand and Ohayon, 1995), which is based on the positive functional:

$$K(\psi) = \frac{\int_{Q_0} (\nabla \psi)^2 \mathrm{d}Q}{\int_{\sum_0} \psi^2 \mathrm{d}S} \tag{6}$$

under the supplementary condition $\int_{\sum_0} \psi \, \mathrm{d}S = 0$. In that case, the absolute minimum of the functional equation (6) coincides with the lowest eigenvalue of the spectral problem (4). Furthermore, the necessary condition for an extrema of equation (6) leads to the variational equation:

$$\int_{Q_0} (\nabla \psi, \nabla \eta) \mathrm{d}Q - \kappa \int_{\sum_0} \psi \eta \mathrm{d}S = 0 \tag{7}$$

with respect to a non-constant function ψ, where η is a smooth test-function.

Variational problem (7) may be solved by the Ritz-Treftz variational scheme. Approximate solutions are then posed as the following linear combination of smooth harmonic functions:

$$\psi(x,y,z) = \sum_{k=1}^{q} a_k B_k(x,y,z). \tag{8}$$

Substituting equation (8) into equation (7) and using $B_i(i = 1, \ldots, q)$ as test-functions, one obtains the spectral matrix problem:

$$\sum_{k=1}^{q} (\{\alpha_{ik}\} - k\{\beta_{ik}\}) a_k = 0, \quad i = 1, \ldots, q \tag{9}$$

Here, the elements of the non-negative matrices $A = \{\alpha_{ik}\}, \ B = \{\beta_{ik}\}$ are computed by the formulae:

$$\alpha_{ik} = \int_{Q_0} (\nabla B_i, \nabla B_k) \mathrm{d}Q = \int_{\sum_0 + S} \frac{\partial B_i}{\partial n} B_j \, \mathrm{d}S, \quad \beta_{ik} = \int_{\sum_0} B_i B_k \mathrm{d}S, \tag{10}$$

and the approximate eigenvalues are roots of the equation:

$$\det(A - \kappa B) = 0, \tag{11}$$

which appears as the necessary solvability condition of system (9). By increasing the dimension q the non-zero roots of equation (11) converge (from above) to the lower eigenvalues of equation (4). Approximate eigenfunctions (8) are formed by the eigenvectors of equation equation (9), $\{a_k, k = 1, \ldots, q\}$.

A key difficulty of the Ritz-Treftz scheme consists of establishing a suitable analytical functional basis $\{B_\mathrm{k}\}$. The completeness of functional sets significantly depends on the actual shape of Q_0. To the author's knowledge, there are two types of analytical functional sets, which may be adapted to the studied case. The first set is proposed in the book by Lukovsky *et al.* (1984). It follows from a separation of variables in the Laplace equation done in the spherical coordinate system. These harmonic solutions are of polynomial structure (harmonic polynomial solutions, HPS) in the Cartesian coordinate system. Their completeness is proved for all star-shaped domains with respect to the origin. Being rewritten in a cylindrical coordinate system, the HPS admit the separation of the angular coordinate and keep polynomial structure with regard to the remaining coordinates, i.e. in projections on a meridional cross-section. A specific functional basis (SFB) is presented by Gavrilyuk *et al.* (2005). It is derived in the cylindrical coordinate system combined with a non-conformal mapping of the meridional cross-section. The functional set is harmonic and satisfies the zero-Neumann condition on the conical walls. Furthermore, we utilise these two functional sets in the Ritz-Treftz scheme to solve the spectral problem (4). The tree-dimensional problem and its variational formulation (7) are thereby reduced to two dimensions by separating the angular-type variable.

3. Ritz-Treftz method based on the HPS

We use the cylindrical coordinate system (X, ξ, η) linked with the original Cartesian coordinates by:

$$x = X + X_0, \quad y = \xi \cos \eta, \quad z = \xi \sin \eta. \tag{12}$$

Here, the lag X_0 along the vertical axis is introduced to superpose the origin of the cylindrical coordinate system with the waterplane. The solution of equation (4) is represented in the following form:

$$\psi(X, \xi, \eta) = \varphi_m(X, \xi) \begin{pmatrix} \sin m\eta \\ \cos m\eta \end{pmatrix}, \quad m = 0, 1, 2 \ldots \tag{13}$$

This makes it possible to separate the angular coordinate η and to reduce the three-dimensional boundary value problem (4) to the following m-parametric family (m is a non-negative integer) of two-dimensional spectral problems:

$$\frac{\partial}{\partial X}\left(\xi\frac{\partial\varphi_m}{\partial X}\right)+\frac{\partial}{\partial\xi}\left(\xi\frac{\partial\varphi_m}{\partial\xi}\right)-\frac{m^2}{\xi}\varphi_m=0\,\text{in}\,G;\quad\frac{\partial\varphi_m}{\partial X}=\kappa_m\varphi_m\,\text{on}\,\mathrm{L}_0;$$
$$\frac{\partial\varphi_m}{\partial n}=0\,\text{on}\,L;\quad|\varphi_\mathrm{m}(X,0)|<\infty;\quad\int_{L_0}\xi\frac{\partial\varphi_0}{\partial X}\,\mathrm{d}\xi=0. \tag{14}$$

Problem (14) is defined in a meridional plane of $Q_0$and $L=L_1+L_2$ (Figure 2). This means that the eigenvalues of the original three-dimensional problem constitute a two-parametric set $\kappa=\kappa_{mi}(m=0,1,\ldots;i=1,2,\ldots)$, where $i\geq 1$ enumerates the eigenvalues of equation (14) in ascending order. The corresponding eigenfunctions of equation (4) take the form equation (13) with $\varphi_m=\varphi_{mi}(X,\xi)$.

According to Lukovsky *et al.* (1984), the HPS admit the following form in the meridional plane (after separation of the η-coordinate):

$$w_k^{(m)}(X,\xi)=\frac{2(k-m)!}{(k+m)!}R^kP_k^{(m)}\left(\frac{X}{R}\right),k\geq m,\quad R=\sqrt{X^2+\xi^2}, \tag{15}$$

Where $P_k^{(m)}$are Legendre's functions of first kind. The functions $\{w_k^{(m)}\}$are the solutions of the first equation of (14). It can be shown that $w_k^{(m)}$ has indeed a polynomial structure in terms of X and ξ. The first functions of the set equation (15) take the form:

$$w_0^{(0)}=1,\quad w_1^{(0)}=X,\quad w_2^{(0)}=X^2-\frac{\xi^2}{2},\quad\ldots\quad(m=0),$$
$$w_1^{(1)}=\xi,\quad w_2^{(1)}=X\xi,\quad w_3^{(1)}=X^2\xi-\frac{\xi^3}{4},\quad\ldots\quad(m=1),$$
$$w_2^{(2)}=\xi^2,\quad w_3^{(2)}=X\xi^2,\quad w_4^{(2)}=X^2,\xi^2-\frac{\xi^4}{6},\quad\ldots\quad(m=2),$$
$$w_3^{(3)}=\xi^3,\quad w_4^{(3)}=X\xi^3,\quad w_5^{(3)}=X^2,\xi^3-\frac{\xi^5}{8},\quad\ldots\quad(m=3).$$

The computation of $\{w_k^{(m)}\}$ can be realised by the following recurrence relations:

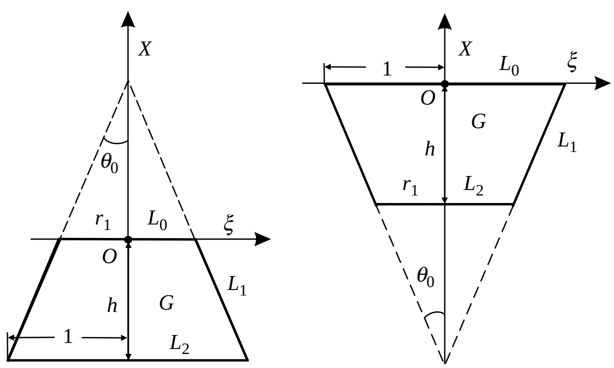

Figure 2.
Meridional planes of Λ- and V-shaped tanks

$$\frac{\partial w_k^{(m)}}{\partial X} = (k-m) w_{k-1}^{(m)}; \quad \xi \frac{\partial w_k^{(m)}}{\partial \xi} = k w_k^{(m)} - (k-m) X w_{k-1}^{(m)},$$

$$(k-m+1) w_{k+1}^{(m)} + (2k+1) X w_k^{(m)} - (k-m)(X^2+\xi^2) w_{k-1}^{(m)},$$

$$(k-m+1)\xi w_k^{(m+1)} = 2(m+1)\big((X^2+\xi^2) w_{k-1}^{(m)} - X w_k^{(m)}\big).$$

By separating the η-coordinate in the variational formulation (7) and in the representation equation (8), we arrive at the following m-parametric families (m is non-negative integer) of approximate solutions:

$$\varphi_m(X,\xi) = \sum_{k=1}^{q} a_k^{(m)} w_{k+m-1}^{(m)}(X,\xi), \tag{16}$$

and spectral matrix problems:

$$\begin{aligned} &\sum_{k=1}^{q} \left(\{\alpha_{ik}^{(m)}\} - \kappa_m \{\beta_{ik}^{(m)}\} \right) a_k = 0 \ \ (i = 1, \ldots, q), \\ &\det\left(\{\alpha_{ik}^{(m)}\} - \kappa_m \{\beta_{ik}^{(m)}\} \right) = 0, \end{aligned} \tag{17}$$

following from (9). The elements $\{\alpha_{ik}^{(m)}\}$and $\{\beta_{ik}^{(m)}\}$are computed for the Λ-cones by the formulae:

$$\alpha_{ij}^{(m)} = \int_0^{r_1} \left(\xi \frac{\partial w_{i+m-1}^{(m)}}{\partial X} w_{j+m-1}^{(m)} \right)_{X=0} \mathrm{d}\xi + \int_{-h}^{0} \left(\xi \frac{\partial w_{i+m-1}^{(m)}}{\partial \xi} w_{j+m-1}^{(m)} \right)_{\xi=\tan\theta_0 X - r_1} \mathrm{d}X$$
$$- \tan\theta_0 \int_{-h}^{0} \left(\xi \frac{\partial w_{i+m-1}^{(m)}}{\partial X} w_{j+m-1}^{(m)} \right)_{\xi=\tan\theta_0 X - r_1} \mathrm{d}X - \int_0^{1} \left(\xi \frac{\partial w_{i+m-1}^{(m)}}{\partial X} w_{j+m-1}^{(m)} \right)_{X=-h} \mathrm{d}\xi,$$

$$\beta_{ij}^{(m)} = \int_0^{r_1} \left(\xi w_{i+m-1}^{(m)} w_{j+m-1}^{(m)} \right)_{X=0} \mathrm{d}\xi,$$

and for the V cones by the formulae:

$$\alpha_{ij}^{(m)} = \int_0^{1} \left(\xi \frac{\partial w_{i+m-1}^{(m)}}{\partial X} w_{j+m-1}^{(m)} \right)_{X=0} \mathrm{d}\xi + \int_{-h}^{0} \left(\xi \frac{\partial w_{i+m-1}^{(m)}}{\partial \xi} w_{j+m-1}^{(m)} \right)_{\xi=\tan\theta_0 X + 1} \mathrm{d}X$$
$$- \tan\theta_0 \int_{-h}^{0} \left(\xi \frac{\partial w_{i+m-1}^{(m)}}{\partial X} w_{j+m-1}^{(m)} \right)_{\xi=\tan\theta_0 X + 1} \mathrm{d}X - \int_0^{r_1} \left(\xi \frac{\partial w_{i+m-1}^{(m)}}{\partial X} w_{j+m-1}^{(m)} \right)_{X=-h} \mathrm{d}\xi,$$

$$\beta_{ij}^{(m)} = \int_0^{1} \left(\xi w_{i+m-1}^{(m)} w_{j+m-1}^{(m)} \right)_{X=0} \mathrm{d}\xi.$$

For each fixed m, the second equation of (17) has q positive roots ($n = 1,2,\ldots,q$). The multiplicity should be accounted for. Since the Ritz-Treftz method implies the minimisation of a functional, the approximate values κ_{mn} converge from above. This makes it possible to check the convergence by the number of significant digits, which do not change as increases. The method gives the best approximation for the lowest eigenvalue κ_{m1}.

Convergence. Our numerical experiments were primary dedicated to eigenvalues κ_{m1}, $m = 0,1,2,3$. These eigenvalues are responsible for the lowest natural modes, which give a decisive contribution to hydrodynamic loads (Ibrahim, 2005; Gavrilyuk *et al.*, 2005). In the case of V-tanks, the method shows a fast convergence to κ_{m1} and provides satisfactory accuracy for κ_{m2} and κ_{m3}, too. It shows a slower convergence for the Λ-tanks. Furthermore, the convergence depends not only on the tank type (V or Λ-shaped), but also on the semi-apex angle $\theta_0$and the dimensionless parameter $0 < r_1 < 1$. The results in Table I (A) exhibit a typical convergence behaviour for the V-tanks with $10° \leq \theta_0 \leq 75°$ and $0.2 \leq r_1 \leq 0.9$. The table shows stabilisation of 5-6 significant digits as $q \geq 14$. The best accuracy is established for the lowest spectral parameter κ_{11}. The accuracy grows with q for $m \neq 0$. However, computations of the value κ_{01}, which is responsible for the axial-symmetric natural mode, may become unstable for $q > 17$. This explains why we do not present numerical results on this eigenvalue for $q = 20$ While $m \neq 1$ and $0.2 \leq r_1 \leq 0.9$, increasing $\theta_0 > 75°$ leads to a slower convergence. In this case, $q = 17,\ldots,20$ guarantees only 3-4 significant digits (necessary engineering accuracy). The same number of basic functions keeps this number of significant digits for the tanks with $r_1 < 0.2$ and $10° \leq \theta_0 \leq 75°$. When r_1 tends to zero (truncated tank is close to a non-truncated one), the approximations κ_{m1} were validated by numerical results reported by Gavrilyuk *et al.* (2005) as well as by experimental data given in Bauer (1982).

In Table I (B), typical convergence behaviour for the Λ-shaped tanks with $10° \leq \theta_0 \leq 75°$ is presented. A comparative analysis of parts (A) and (B) illustrates that the method is in the latter case less efficient. In particular, computations of κ_{01} are not so precise. Moreover, 18-20 basic functions lead to 4-5 significant digits of κ_{m1} only for $r_1 \geq 0.4$. This is not the case for lower values of r_1. Furthermore, when $r_1 \leq 0.2, q = 17,\ldots,20$ can only guarantee 2-3 significant digits for κ_{11}. The slower convergence for the Λ-shaped tanks can in part be clarified by the occurrence of singular first derivatives of the eigenfunctions ψ_m at an inner vertex between $L_0$and L_1 (see the mathematical results by Lukovsky *et al.*, 1984). The HPS are smooth in the (ξ, X)-plane, and, therefore, do not capture this singular behaviour. The singularity disappears when the corner angle is less than 90°. This occurs only for the Λ-shaped tanks. The V-shaped tanks are characterised by a similar singularity at the vertex formed by $L_1$and L_2. However, because the natural modes (eigenfunctions ψ_m) should “decay” exponentially downward, the method may be sensitive with respect to that singularity only for shallow water. Our numerical experiments confirm this fact as$r_1 < 0.1$.

3.1 Ritz-Treftz method based on the SFB

The nonlinear resonant sloshing is effectively studied by multimodal methods. As it is shown by Lukovsky (1975), Lukovsky and Timokha (2002), these methods require analytical expressions for the natural modes, which:

Table I. Convergence to $\kappa_{m1}, m = 0,1,2,3$ for different r_1 versus the number of basic functions q (16)

	A						B				
q	$r_1 = 0.2$	$r_1 = 0.4$	$r_1 = 0.6$	$r_1 = 0.8$	$r_1 = 0.9$	Q	$r_1 = 0.2$	$r_1 = 0.4$	$r_1 = 0.6$	$r_1 = 0.8$	$r_1 = 0.9$
κ_{01}											
2	5.032415	4.577833	4.1523522	3.805501	2.961399	8	70.06337	15.14094	6.899986	4.5609911	2.683411
5	3.394779	3.392286	3.384865	3.141171	2.200342	10	50.46762	11.12449	6.672266	4.551150	2.683117
8	3.385603	3.385592	3.381845	3.138861	2.197438	12	39.06111	10.18563	6.666704	4.550877	2.682932
11	3.385600	3.385590	3.381827	3.138718	2.197238	14	32.07572	10.01745	6.665678	4.550590	2.682796
14	3.385600	3.385590	3.381822	3.138665	2.197162	16	27.64904	10.01612	6.665058	4.550422	2.682751
17	3.385600	3.385590	3.381819	3.138644	2.197138	18	25.15299	10.01426	6.664886	4.550349	2.682730
						κ_{11}					
2	1.343631	1.335723	1.299977	1.007261	0.607340	8	16.50485	5.694833	3.516782	1.661815	0.726555
5	1.304413	1.301793	1.254157	0.934412	0.542503	10	13.94781	5.633730	3.515861	1.661684	0.726507
8	1.304378	1.301694	1.254054	0.933885	0.542284	12	13.48767	5.631904	3.515547	1.661608	0.726489
11	1.304377	1.301692	1.253982	0.933835	0.542257	14	12.24724	5.630560	3.515365	1.661559	0.726484
14	1.304377	1.301687	1.253972	0.933823	0.542251	16	11.66350	5.629898	3.515269	1.661551	0.726482
17	1.304377	1.301686	1.253969	0.933819	0.542249	18	11.45072	5.629777	3.515237	1.661537	0.726480
20	1.304377	1.301686	1.253967	0.933817	0.542248	20	11.33183	5.629888	3.515214	1.661532	0.726478
						κ_{21}					
2	2.443739	2.424390	2.86633	2.191371	1.572048	8	45.02411	9.797804	5.950925	3.724251	1.923234
5	2.263550	2.263351	2.255096	2.015602	1.361905	10	28.65250	9.096131	5.941913	3.724049	1.923019
8	2.263151	2.263087	2.255004	2.014923	1.360928	12	25.18394	8.975383	5.941107	3.723708	1.922950
11	2.263150	2.263087	2.254976	2.014838	1.360837	14	24.77166	8.968027	5.941002	3.723640	1.922930
14	2.263150	2.263086	2.254972	2.014811	1.360805	16	21.51273	8.966657	5.940651	3.723591	1.922913
17	2.263150	2.263086	2.254969	2.014801	1.360795	18	19.73858	8.966531	5.940603	3.723549	1.922899
20	2.263150	2.263086	2.254968	2.014796	1.360790	20	17.76023	8.966524	5.940589	3.723542	1.922895
						κ_{31}					
2	3.533170	3.520882	3.459048	3.316198	2.697426	8	139.8798	15.67055	8.146078	5.634069	3.404035
5	3.181530	3.181299	3.179541	3.047179	2.329022	10	83.82254	12.95492	8.046749	5.633996	3.403568
8	3.180251	3.180249	3.179080	3.046742	2.327044	12	64.58853	12.22964	8.044916	5.633565	3.403460
11	3.180249	3.180248	3.179077	3.046654	2.326812	14	53.41076	12.08855	8.044459	5.633498	3.403411
14	3.180249	3.180247	3.179074	3.046620	2.326812	16	53.13873	12.07964	8.044234	5.633377	3.403360
17	3.180249	3.180247	3.179073	3.046606	2.326790	18	38.85519	12.08400	8.044028	5.633343	3.40336
20	3.180249	3.180247	3.179073	3.046599	2.326779	20	36.46749	12.08490	8.043988	5.633321	3.403328

Notes: Column (A) is for a V-shaped tank, (B) corresponds to a Λ-shaped tank, $\theta_0 = 30°$

- are analytically expandable over the waterplane;
- satisfy a zero-Neumann condition at the tank walls and, if the tank is non-cylindrical; and
- can be transformed to a curvilinear coordinate system (x_1,x_2,x_3), in which the free surface is governed by the normal form representation $x_1 = f(x_2, x_3, t)$.

An example of suitable approximate natural modes for non-truncated V-tanks is given by Lukovsky (1990) and Gavrilyuk *et al.* (2005). The present section generalises these results.

Curvilinear coordinate system. The non-Cartesian parametrisation proposed by Gavrilyuk et al (2005) links the x,y,z coordinates with x_1,x_2,x_3 as follows:

$$x = x_1, \quad y = x_1 x_2 \cos x_3, \quad z = x_1 x_2 \sin x_3. \tag{18}$$

Thus, the variable $x_3 = \eta$ is the polar angle in the Oyz-plane and corresponds to η in equation (12). Figure 3 demonstrates that the hydrostatic liquid domain Q_0 takes in the (x_1,x_2,x_3)-system the form of an upright rectangular base cylinder ($x_0 \leq x_1 \leq x_{10}, 0 \leq x_2 \leq x_{20}, 0 \leq x_3 \leq 2\pi$). The domain $G*$ represents a rectangle with the sides $h = x_{10} - x_0$and $x_{20} = \tan\theta_0$ in theOx_2x_1-plane. Here, the radius of the undisturbed water plane is $r_t = 1$ for the V-tanks and$r_t = r_1$ for the Λ-tanks. Having presented:

$$\varphi(x_1, x_2, x_3) = \psi_m(x_1, x_2)\begin{pmatrix} \sin m\,x_3 \\ \cos m\,x_3 \end{pmatrix}, \quad m = 0, 1, 2, \ldots \tag{19}$$

and following Gavrilyuk *et al.* (2005), one obtains that the original three-dimensional problem (4) admits separation of the spatial variable x_3. Furthermore, the transformation (18) generates the following m-parametric family of spectral problems with respect to:

$$p\frac{\partial^2\psi_m}{\partial x_1^2} + 2q\frac{\partial^2\psi_m}{\partial x_1\partial x_2} + s\frac{\partial^2\psi_m}{\partial x_2^2} + \mathrm{d}\frac{\partial\psi_m}{\partial x_2} - m^2 c\psi_m = 0 \quad \text{in} \quad G^*, \tag{20}$$

$$p\frac{\partial\psi_m}{\partial x_1} + q\frac{\partial\psi_m}{\partial x_2} = \kappa_m p\psi_m \quad \text{on} \quad \mathscr{L}_0^*, \tag{21}$$

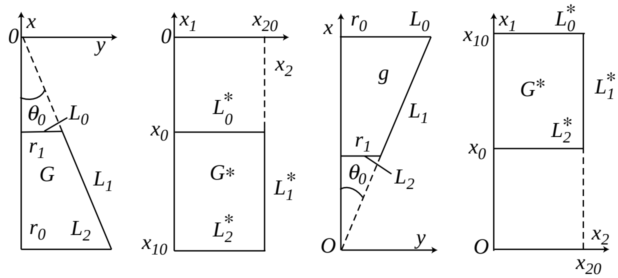

Figure 3.
Meridional cross-sections of the original and transformed domains

$$s\frac{\partial\psi_m}{\partial x_2}+q\frac{\partial\psi_m}{\partial x_1}=0 \quad \text{on} \quad \mathscr{L}_1^*, \tag{22}$$

$$p\frac{\partial\psi_m}{\partial x_1}+q\frac{\partial\psi_m}{\partial x_2}=0 \quad \text{on} \quad \mathscr{L}_2^*, \tag{23}$$

$$|\psi_m(x_1,0)|<\infty, \quad m=0,1,2,\ldots, \tag{24}$$

$$\int_0^{x_20}\psi_0 x_2 \mathrm{d}x_2=0, \tag{25}$$

where $G*=\{(x_1,x_2): x_0\leq x_1\leq x_{10}, 0\leq x_2\leq x_{20}\}$, $\bar{W}_k^{(0)}$, $\mathrm{d}=1+2x_2^2, c=1/x_2$ and the boundary of G^* consists of the portions $\mathscr{L}_0^*, \mathscr{L}_1^*$ and $\mathscr{L}_2^*$.

Particular solutions of equation (20) and equation(22). Gavrilyuk *et al.* (2005) studied a spectral problem, which is similar to equations (20)-(25). Following results by Eisenhart, they proved that equation (20) and equation (22) allow together for the separation of the spatial variables x_1 and x_2. For our problem, this separation leads to the following particular solutions:

$$x_1^\nu T_\nu^{(m)}(x_2) \quad \text{and} \quad \frac{\overline{T}_\nu^{(m)}(x_2)}{x_1^{1+\nu}}, \quad \nu\geq 0. \tag{26}$$

In order to determine $T_\nu^{(m)}$, we have to consider the following homogeneous boundary value problem, which depends on the real parameter ν:

$$x_2^2(1+x_2^2)T_\nu^{''(m)}+x_2(1+2x_2^2-2\nu x_2^2)T_\nu^{''(m)}+[\nu(\nu-1)x_2^2-m^2]T_\nu^{(m)}=0, \tag{27}$$

$$T_\nu^{''(m)}(x_{20})=\nu\frac{x_{20}}{1+x_{20}^2}\,T_\nu^{(m)}(x_{20}), \quad |T_\nu^{(m)}(0)|<\infty. \tag{28}$$

It can be shown that the problem (27) and (28) has only nontrivial solutions for a countable set of values $\nu=\nu_{mn}\geq 0 (m=0,1,\ldots; n=1,2,\ldots)$.

The second class of functions, $\overline{T}_\nu^{(m)}$, appears only in the case of $x_0\neq 0$, i.e. when the conical tank is truncated. Computation of $\overline{T}_\nu^{(m)}$ leads to the following ν-parametric problem:

$$x_2^2(1+x_2^2)\overline{T}^{''(m)}+x_2(1+4x_2^2-2\nu x_2^2)\overline{T}'_\nu+[(\nu+1)(\nu+2)x_2^2-m^2]\overline{T}^{(m)}=0, \tag{29}$$

$$\overline{T}'^{(m)}(x_{20})+(\nu+1)\frac{x_{20}}{1+x_{20}^2}\overline{T}^{(m)}(x_{20})=0. \tag{30}$$

Obviously, nontrivial solutions of equation (29) and equation (30) exist only for a countable set of nonnegative values ν.

Let us now show that the solution of equations (27) and (29) can be expressed in terms of the spheroidal harmonics and the set $\{\nu_{mn}\}$ is the same for the problems (27) and (28) and the problems (29) and (30). For this purpose, we change the variables in equations (27) and (29) by $\mu=(1+x_2^2)^{-(1/2)}$ and substitute $y(\mu)=\mu^\nu T(\mu)$ and

$y(\mu) = \mu^{-1-\nu}\overline{T}(\mu)$ into equation (27) and equation (29), respectively. This reduces the two equations to the same well-known differential equation:

$$(1-\mu^2)y''(\mu) - 2\mu y'(\mu) + \left[\nu(\nu+1) - \frac{m^2}{1-\mu^2}\right]y(\mu) = 0,$$

whose solutions coincide with the Legendre function of first kind, i.e. $y(\mu) = P_\nu^{(m)}(\mu)$.

Furthermore, treating the boundary conditions (28) and (30) in the same way and using the substitution $\mu = \cos\theta$, the following common equation is obtained:

$$\left.\frac{\partial P_\nu^{(m)}(\cos\theta)}{\partial\theta}\right|_{\theta=\theta_0} = 0. \tag{31}$$

This equation can be considered as a transcendental equation for the computation of the values $\{\nu_{mn}\}$- Appendix (Figure A1) presents the first 12 values of $\{\nu_{mn}\}$ $(m = 0,1,2,3)$ versus θ_0.

In conclusion, with the technique described above, we get the following nontrivial particular solutions

$$T_{\nu_{mk}}^{(m)}(x_2) = (1+x_2^2)^{\frac{\nu_{mk}}{2}} P_{\nu_{mk}}^{(m)}\left(\frac{1}{\sqrt{1+x_2^2}}\right), \tag{32}$$

$$\overline{T}_{\nu_{mk}}^{(m)}(x_2) = (1+x_2^2)^{\frac{-1-\nu_{mk}}{2}} P_{\nu_{mk}}^{(m)}\left(\frac{1}{\sqrt{1+x_2^2}}\right). \tag{33}$$

Particular solutions as a functional basis. Let the particular solutions (26), (32) and (33) be rewritten in the form:

$$W_k^{(m)}(x_1,x_2) = N_k^{(m)} x_1^{\nu_{mk}} T_{\nu_{mk}}^{(m)}(x_2), \quad \bar{W}_k^{(m)}(x_1,x_2) = \bar{N}_k^{(m)} x_1^{-1-\nu_{mk}} \overline{T}_{\nu_{mk}}^{(m)}(x_2). \tag{34}$$

Here, $N_k^{(m)}$ and $\bar{N}_k^{(m)}$ are multipliers which are chosen to satisfy the following condition:

$$\begin{aligned} 1 &= \|W_k^{(m)}\|^2_{\mathscr{L}_2^*+\mathscr{L}_0^*} = \|\bar{W}_k^{(m)}\|^2_{\mathscr{L}_2^*+\mathscr{L}_0^*} \\ &= \int_0^{x_{20}} x_2[(W_k^{(m)}|_{x_1=x_{10}})^2 + (W_k^{(m)}|_{x_1=x_0})^2]\mathrm{d}x_2 \\ &= \int_0^{x_{20}} x_2[(\bar{W}_k^{(m)}|x_1 = x_{10})^2 + (\bar{W}_k^{(m)}|_{x_1=x_0})^2]\mathrm{d}x_2. \end{aligned} \tag{35}$$

equation (35) says that $W_k^{(m)}$ and $\bar{W}_k^{(m)}$. have the unit norm (in the mean-squares metrics) on the boundary $\mathscr{L}_2^* + \mathscr{L}_0^*$, where equations (21) and (23) should be approximately satisfied. Explicit formulae for these normalising multipliers have the form:

$$N_k^{(m)} = \frac{1}{\sqrt{x_{10}^{2\nu_{mk}} + x_0^{2\nu_{mk}}}} \frac{1}{\sqrt{\int_0^{x_{20}} (1+x_2^2)^{\nu_{mk}} \left(P_{\nu_{mk}}^{(m)}\right)^2 \mathrm{d}x_2}},$$

$$\bar{N}_k^{(m)} = \frac{1}{\sqrt{x_{10}^{-2-2\nu_{mk}} + x_0^{-2-2\nu_{mk}}}} \frac{1}{\sqrt{\int_0^{x_{20}} (1+x_2^2)^{-1-\nu_{mk}} \left(P_{\nu_{mk}}^{(m)}\right)^2 \mathrm{d}x_2}}.$$

The case $m = 0$ requires, in addition, the volume conservation condition (25). This implies a re-definition of the functions $W_k^{(0)}$ and $\bar{W}_k^{(0)}$ by: $W_k^{(0)} := W_k^{(0)} - c_k^{(0)}$, $\bar{W}_k^{(0)} := \bar{W}_k^{(0)} - \bar{c}_k^{(0)}$,where:

$$c_k^{(0)} = \frac{2}{x_{20}^2} \int_0^{x_{20}} x_2 W_k^{(0)}(x_{10}, x_2)\mathrm{d}x_2, \quad \bar{c}_k^{(0)} = \frac{2}{x_{20}^2} \int_0^{x_{20}} x_2 \bar{W}_k^{(0)}(x_{10}, x_2)\mathrm{d}x_2.$$

Variational method. In accordance with the Ritz-Treftz scheme, we represent approximate solutions of equations (20)-(25) in the form:

$$\psi_m(x_1, x_2) = \sum_{k=1}^{q_1} a_k^{(m)} W_k^{(m)} + \sum_{l=1}^{q_2} \bar{a}_l^{(m)} \bar{W}_l^{(m)}. \tag{36}$$

By separating the x_3 coordinate in variational formulation (7) (after substitution of equation (19)), representation (36) leads to the m-parametric family of spectral problems:

$$\begin{gathered} \sum_{k=1}^{Q} \left(\left\{ \alpha_{ik}^{(m)} \right\} - \kappa_m \left\{ \beta_{ik}^{(m)} \right\} \right) \alpha_k = 0 \quad (i = 1, \ldots, Q), \\ \det \left(\left\{ \tilde{\alpha}_{ij}^{(m)} \right\} - \kappa_m \left\{ \tilde{\beta}_{ik}^{(m)} \right\} \right) = 0. \end{gathered} \tag{37}$$

The spectral problem (37) has $Q = q_1 + q_2$ eigenvalues. Because the representation (36) contains two types of functions, namely $W_k^{(m)}$ and, $\bar{W}_l^{(m)}$there exist four sub-matrices of $\left\{\tilde{\alpha}_{ij}^{(m)}\right\}$ and $\left\{\tilde{\beta}_{ij}^{(m)}\right\}$ such that:

$$\tilde{\alpha}_{ij}^{(m)} = \begin{pmatrix} \alpha_{ij1}^{(m)} & \alpha_{ij2}^{(m)} \\ \alpha_{ij3}^{(m)} & \alpha_{ij4}^{(m)} \end{pmatrix}, \quad \tilde{\beta}_{ij}^{(m)} = \begin{pmatrix} \beta_{ij1}^{(m)} & \beta_{ij2}^{(m)} \\ \beta_{ij3}^{(m)} & \beta_{ij4}^{(m)} \end{pmatrix}.$$

The elements $\left\{\alpha_{ijs}^{(m)}\right\}$ and $\left\{\beta_{ijs}^{(m)}\right\}$, $s = 1, \ldots, 4$, are computed by the formulae:

$$\alpha_{ij1}^{(m)} = \int_0^{x_{20}} \left(x_1^2 x_2 \frac{\partial W_i^{(m)}}{\partial x_1} - x_1 x_2^2 \frac{\partial W_i^{(m)}}{\partial x_2} \right)_{x_1 = h_t} W_j^{(m)} \mathrm{d}x_2$$

$$- \int_0^{x_{20}} \left(x_1^2 x_2 \frac{\partial W_i^{(m)}}{\partial x_1} - x_1 x_2^2 \frac{\partial W_i^{(m)}}{\partial x_2} \right)_{x_1 = h_b} W_j^{(m)} \mathrm{d}x_2,$$

$$\alpha_{ij2}^{(m)} = \int_0^{x_{20}} \left(x_1^2 x_2 \frac{\partial W_i^{(m)}}{\partial x_1} - x_1 x_2^2 \frac{\partial W_i^{(m)}}{\partial x_2} \right)_{x_1=h_t} \bar{W}_j^{(m)} \mathrm{d}x_2$$

$$- \int_0^{x_{20}} \left(x_1^2 x_2 \frac{\partial W_i^{(m)}}{\partial x_1} - x_1 x_2^2 \frac{\partial W_i^{(m)}}{\partial x_2} \right)_{x_1=h_b} \bar{W}_j^{(m)} \mathrm{d}x_2,$$

$$\alpha_{ij3}^{(m)} = \int_0^{x_{20}} \left(x_1^2 x_2 \frac{\partial \bar{W}_i^{(m)}}{\partial x_1} - x_1 x_2^2 \frac{\partial \bar{W}_i^{(m)}}{\partial x_2} \right)_{x_1=h_t} W_j^{(m)} \mathrm{d}x_2$$

$$- \int_0^{x_{20}} \left(x_1^2 x_2 \frac{\partial \bar{W}_i^{(m)}}{\partial x_1} - x_1 x_2^2 \frac{\partial \bar{W}_i^{(m)}}{\partial x_2} \right)_{x_1=h_b} W_j^{(m)} \mathrm{d}x_2,$$

$$\alpha_{ij4}^{(m)} = \int_0^{x_{20}} \left(x_1^2 x_2 \frac{\partial \bar{W}_i^{(m)}}{\partial x_1} - x_1 x_2^2 \frac{\partial \bar{W}_i^{(m)}}{\partial x_2} \right)_{x_1=h_t} \bar{W}_j^{(m)} \mathrm{d}x_2$$

$$- \int_0^{x_{20}} \left(x_1^2 x_2 \frac{\partial \bar{W}_i^{(m)}}{\partial x_1} - x_1 x_2^2 \frac{\partial \bar{W}_i^{(m)}}{\partial x_2} \right)_{x_1=h_b} \bar{W}_j^{(m)} \mathrm{d}x_2,$$

$$\beta_{ij1}^{(m)} = h_t^2 \int_0^{x_{20}} x_2 \left(W_i^{(m)} W_j^{(m)} \right)_{x_1=h_t} \mathrm{d}x_2, \quad \beta_{ij2}^{(m)} = h_t^2 \int_0^{x_{20}} x_2 \left(W_i^{(m)} \bar{W}_j^{(m)} \right)_{x_1=h_t} \mathrm{d}x_2,$$

$$\beta_{ij3}^{(m)} = h_t^2 \int_0^{x_{20}} x_2 \left(\bar{W}_i^{(m)} W_j^{(m)} \right)_{x_1=h_t} \mathrm{d}x_2, \quad \beta_{ij4}^{(m)} = h_t^2 \int_0^{x_{20}} x_2 \left(\bar{W}_i^{(m)} \bar{W}_j^{(m)} \right)_{x_1=h_t} \mathrm{d}x_2.$$

In the case of Λ- and V-tanks, we have $h_t = r_1/\tan\theta_0$, $h_b = 1/\tan\theta_0$ and $h_t = 1/\tan\theta_0$, $h_b = r_1/\tan\theta_0$, respectively.

Convergence. Column A in Table II shows a typical convergence behaviour in the case of V-tanks with $10° \le \theta_0 \le 75°$ and $0.2 \le r_1 \le 0.9$. When $0.2 \le r_1 \le 0.55$, the method generates 4-5 significant digits of κ_{m1} for $q = q_1 = q_2 = 7, \ldots, 10$ ($14, \ldots, 20$ basic functions). This is consistent with the convergence results in Section 3. However, the SFB keeps also a fast convergence to κ_{m1} for $r_1 < 0.2$. This includes the case of κ_{01}, which has not been satisfactory handled by the HPS. Moreover, when $0 < r_1 \le 0.4$, the number of significant digits is larger (for the same number of basic functions) for $15° \le \theta_0 < 30°$, but it is only marginally smaller for $15° \le \theta_0$. Gavrilyuk *et al.* (2005) related such a slower convergence of an analogous method for smaller semi-apex angles to the asymptotic behaviour of the exact solution along the vertical axis. Their conclusion is that the eigenfunctions ψ_{m} should exponentially decay downward Ox for a circular cylindrical tank, to which the conical domain tends as θ_0 decreases. However, $W_k^{(m)}$ and $\bar{W}_k^{(m)}$ do not capture this decaying. Furthermore, decreasing the dimensionless liquid depth $h(r_1 \to 1$ or $\theta_0 \to 90°)$ may cause a lower accuracy (3-4 significant digits for 18-24 basic functions).

	A					B				
Q	$r_1 = 0.2$	$r_1 = 0.4$	$r_1 = 0.6$	$r_1 = 0.8$	$r_1 = 0.9$	$r_1 = 0.2$	$r_1 = 0.4$	$r_1 = 0.6$	$r_1 = 0.8$	$r_1 = 0.9$
2	3.385676	3.385666	3.382064	3.148405	2.224870	20.82985	10.41489	6.934470	4.781070	2.868894
3	3.385606	3.385596	3.381920	3.143923	2.211744	20.29240	10.14616	6.754682	4.629653	2.748954
4	3.385601	3.385591	3.381878	3.141937	2.206179	20.15184	10.07588	6.707583	4.588863	2.715911
5	3.385600	3.385590	3.381859	3.140888	2.203283	20.09711	10.04852	6.689248	4.572788	2.702514
6	3.385600	3.385590	3.381847	3.140267	2.201583	20.07070	10.03531	6.680396	4.264916	2.695817
7	3.385600	3.385590	3.381840	3.139870	2.200501	20.05610	10.02801	6.675501	4.560515	2.692006
8	3.385600	3.385590	3.381835	3.139601	2.199769	20.04724	10.02358	6.672529	4.557819	2.689637
9	3.385600	3.385590	3.381832	3.139410	2.199252	20.04147	10.02070	6.670596	4.556053	2.688066
10	3.385600	3.385590	3.381829	3.139270	2.198872	20.03753	10.01872	6.669272	4.554837	2.686973
11	3.385600	3.385590	3.381827	3.139164	2.198585	20.03471	10.01732	6.668327	4.553964	2.686181
12	3.385600	3.385590	3.381826	3.139082	2.198364	20.03263	10.01628	6.667629	4.553317	2.685590
					κ_{01}					
2	1.304378	1.301707	1.254338	0.935957	0.544861	11.33533	5.647088	3.528677	1.672867	0.732410
3	1.304377	1.301695	1.254148	0.934864	0.543483	11.31577	5.637221	3.521265	1.666870	0.729246
4	1.304377	1.301691	1.254073	0.934437	0.542976	11.30879	5.633703	3.518590	1.664611	0.728093
5	1.304377	1.301689	1.254036	0.934226	0.542729	11.30558	5.632078	3.517343	1.663527	0.727536
6	1.304377	1.301688	1.254016	0.934106	0.542589	11.30384	5.631202	3.516665	1.662926	0.727224
7	1.304377	1.301687	1.254003	0.934032	0.542502	11.30281	5.630678	3.516258	1.662559	0.727032
8	1.304377	1.301687	1.253994	0.933983	0.542445	11.30214	5.630340	3.515995	1.662319	0.726906
9	1.304377	1.301687	1.253988	0.933949	0.542405	11.30168	5.630110	3.51515	1.662153	0.726818
10	1.304377	1.301686	1.253984	0.933924	0.542376	11.30136	5.629947	3.515687	1.662034	0.726754
11	1.304377	1.301686	1.253981	0.933906	0.542354	11.30112	5.629826	3.515592	1.661945	0.726707
12	1.304377	1.301686	1.253978	0.933892	0.542337	11.30094	5.629735	3.515520	1.661878	0.726671
					κ_{21}					
2	2.263162	2.263100	2.255147	2.019323	1.371212	18.03918	9.019177	5.977616	3.761864	1.952759
3	2.263151	2.263088	2.255060	2.017249	1.366295	17.98215	8.990657	5.958186	3.742630	1.938182
4	2.263150	2.263087	2.255026	2.016335	1.364234	17.96014	8.979646	5.950674	3.734876	1.932215
5	2.263150	2.263087	2.255007	2.015850	1.363151	17.94951	8.974330	5.947040	3.731012	1.929167
6	2.263150	2.263086	2.254996	2.015563	1.362510	17.94361	8.971384	5.945023	3.728818	1.927400
7	2.263150	2.263086	2.254989	2.015378	1.362099	17.94003	8.969588	5.943793	3.727457	1.926285
8	2.263150	2.263086	2.254985	2.015252	1.361819	17.93768	8.968417	5.942990	3.726556	1.925537
9	2.263150	2.263086	2.254981	2.015163	1.361620	17.93607	8.967612	5.942438	3.725930	1.925011
10	2.263150	2.263086	2.254979	2.015097	1.361473	17.93492	8.967036	5.942042	3.725477	1.924627
11	2.263150	2.263086	2.254977	2.015047	1.361362	17.93407	8.966610	5.941750	3.725140	1.924338
12	2.263150	2.263086	2.254976	2.015008	1.361276	17.93342	8.966287	5.941527	3.724882	1.924115
					κ_{31}					
2	3.180280	3.180279	3.179147	3.051144	2.346969	24.36124	12.18061	8.115651	5.700453	3.473876
3	3.180251	3.180250	3.179101	3.049247	2.338329	24.25430	12.12714	8.079896	5.667935	3.441587
4	3.180249	3.180248	3.179090	3.048337	2.334334	24.21030	12.10514	8.065186	5.654291	3.427352
5	3.180249	3.180249	3.179085	3.047828	2.332117	24.18824	12.09411	8.057806	5.647308	3.419803
6	3.180249	3.180247	3.179082	3.047514	2.330753	24.17570	12.08787	8.053610	5.643277	3.415319
7	3.180249	3.180247	3.179080	3.047306	2.329853	24.16792	12.08395	8.051009	5.640748	3.412440
8	3.180249	3.180247	3.179078	3.047161	2.329228	24.16278	12.08138	8.049290	5.639061	3.410481
9	3.180249	3.180247	3.179077	3.047056	2.328776	24.15922	12.07960	8.048098	5.637882	3.409090
10	3.180249	3.180247	3.179077	3.046978	2.328438	24.15666	12.07832	8.047239	5.637026	3.408066
11	3.180249	3.180247	3.179076	3.046918	2.328179	24.15475	12.07736	8.046600	5.636386	3.407290
12	3.180249	3.180247	3.179076	3.046871	2.327976	24.15329	12.07664	8.046112	5.635894	3.406689

Notes: Column (A) is for a V-shaped tank; (B) corresponds to a Λ-shaped tank, $\theta_0 = 30°$

Table II. Convergence to κ_{m1}, $m = 0,1,2,3$, for different r_1 versus the number of basic functions $q = q_1 = q_2$ in (36)

Column B in Table II shows convergence for a Λ-tank. The same r_1 and θ_0 as in the column A are chosen. It can be seen that the numerical results may be less precise than those in Section 3. For instance, the same number of basic functions gives only 2-3 significant digits when $0.2 \leq r_1 \leq 0.9$. However, in contrast to the HPS, the SFB provides reliable computations for the case of an axial symmetric mode κ_{01}. In addition, whereas $0.05 \leq r_1 \leq 0.4$, the lowest eigenvalue κ_{11} is calculated with a better accuracy. For the same r_1, increasing the semi-apex angle may lead to a slower convergence. If $q_1 = q_2 = 12$, the number of significant digits also decreases as $r_1 \rightarrow 1$. This "shallow water" case is handled with 2-3 significant digits as $q_1 = q_2 = 12, \ldots, 14$.

The presence of the two types of basic functions in the representation (36) makes it possible to vary q_1 and q_2 to obtain a better approximation with the same total number of basic functions $Q = q_1 + q_2$ Variations of q_1 and q_2 with a fixed $Q \geq 16$ showed that a better accuracy of κ_{m1} can be expected for $q_2 > q_1$. In particular, this is true for smaller liquid depths. For example, when the V-shaped tank is characterised by $\theta_0 = 30°$ and $r_1 = 0.9$, the approximate $\kappa_{11} = 54233738$ can be obtained with either $q_1 = q_2 = 12(Q = 24)$ or $q_1 = 7, q_2 = 12(Q = 19)$.

4. Comparative analysis of the two method

A comparison of numerical experiments performed with the two different functional bases shows, that the method based on the HPS is more accurate for smaller liquid depths ($0.6 \leq r_1$). However, larger liquid depths ($r_1 \leq 0.4$) are better treated with the second method. This can clearly be seen for the Λ-shaped tanks: the calculations with the method by the SFB keep robustness as the number of basic functions is increased, while the first method fails for larger dimensions. Generally speaking, the accuracy of both methods is similar only for V-tanks with $0.2 \leq r_1 \leq 0.55$, $\theta_0 > 10^0$.

Even though the number of basic functions is small, the two proposed methods give an accurate approximation of the lowest eigenvalue κ_{11}. The lowest eigenvalue determines the lowest natural frequency by $\sigma_{11} = \sqrt{g\kappa_{11}}$. This frequency is of primary interest for modelling tower vibrations with a V-shaped tank. Therefore, we placed special emphasis on a comparison of the numerical results obtained by the two methods for κ_{11}. The results are illustrated in Figure 4(a) and (b). Here, domains in the (r_1, θ_0)-plane are identified, for which each of the methods gives the same number of significant digits with twenty basic functions. One can see that the accuracy of the first method (HPS) may become low only for small θ_0 and r_1, e.g. for large liquid depths. In the other cases, the method guarantees a fast convergence and high accuracy. On the other hand, small θ_0

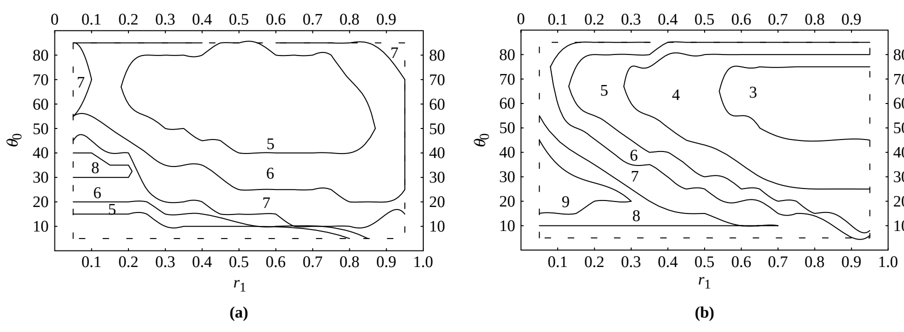

Figure 4.
The number of significant figures of κ_{11} obtained for V-tanks with 20 basic functions by the methods based on the HPS (Case a) and the SF(Case b)

and r_1 are satisfactory handled by the second method (SFB). However, this method converges slowly as $r_1 \to 1$ and $\theta_0 > 45°$, e.g. for small liquid depths.

5. The lowest natural sloshing frequency

The natural sloshing frequencies σ_{m1} are functions of the liquid depth h, the semi-apex angle θ_0 and the radii r_1 and r_0. For the V-tanks, an increasing of $\theta_0$decreases the non-dimensional eigenvalues κ_{m1} (the non-dimensional natural sloshing frequencies $\sigma^2_{m1} r_0/g = \kappa_{m1}$). For the Λ-tanks, an increasing of $\theta_0$increases κ_{m1}.

Dependence of κ_{m1} on the ratio r_1/r_0 is illustrated in Figure 5(a) and (b). These demonstrate that the non-dimensional frequencies decrease as the ratio $r_1/r_0 = (1 + \tan(\theta_0)h/r_1)$ decreases. In term of the fixed dimensional values of r_1 and θ_0, this means that the non-dimensional sloshing frequencies decrease with decreasing the liquid depth h.

One interesting fact is that $\kappa_{01} \approx \kappa_{21}$ for the studied geometric parameters in the case of Λ-tanks. This is the same as for an upright circular cylindrical tank.

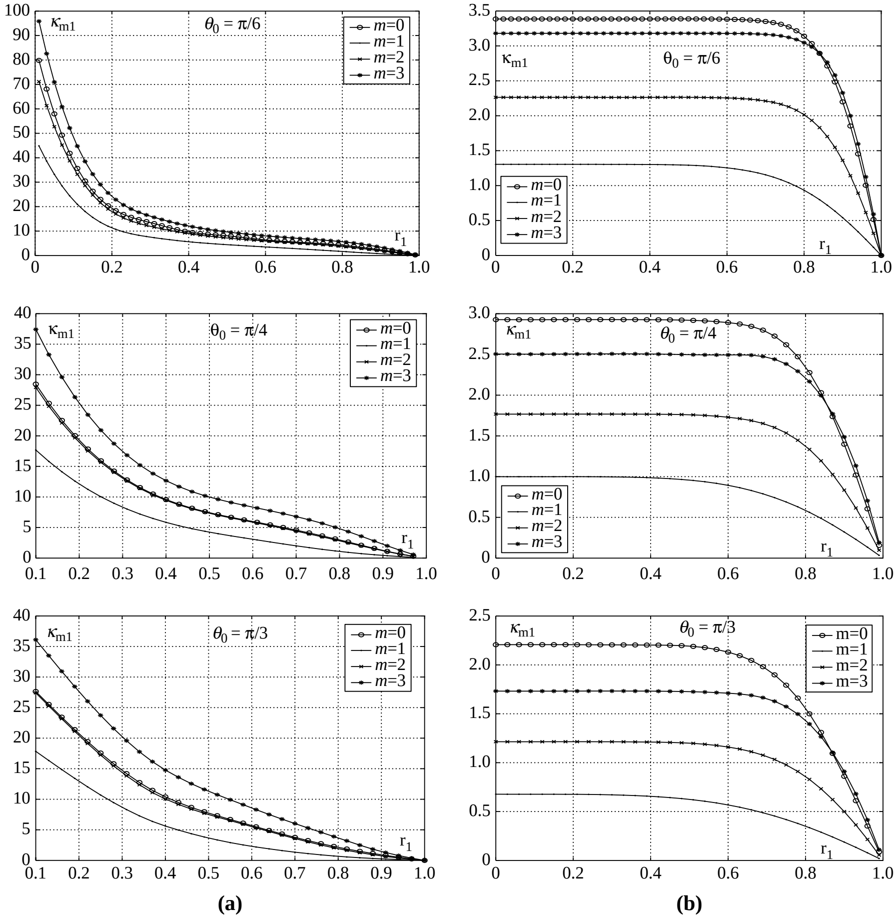

Figure 5.
Eigenvalues κ_{m1} versus r_1 for Λ-shaped (Case a) and V-shaped tanks (Case b)

Further, the natural sloshing frequencies are very close to those for the non-truncated conical V-shape tank as $0 \leq r_1 < 0.6$. Truncation matters for $r_1 \to 1$, i.e. for shallow-water sloshing.

The natural sloshing frequency an σ_{11} of practical importance for the design of water towers (Damatty and Sweedan, 2006). Having in mind this fact, we present in Table III the values of κ_{11} versus $\theta_0$and r_1. The corresponding computations have been done to guarantee up to five significant digits. The dimensional natural sloshing frequency σ_{11} is computed from κ_{11} by the formula:

$$\sigma_{11} = \sqrt{\frac{g\kappa_{11}(\theta_0, r_1/r_0)}{r_0}}, \tag{38}$$

where g and r_1 are not scaled by r_0. The numerical data from Table III can therefore be used in both the structural design and the validation of other numerical methods.

6. Concluding remarks

We have proposed two efficient numerical-analytical methods for the computation of the natural sloshing frequencies and modes in truncated conical tanks. These methods are based on the Ritz-Treftz variational scheme. Extensive numerical experiments showed that these methods have different domains of applicability in terms of the semi-apex angle, the liquid depth and the tank type (V- or Λ-shaped).

The methods may have slow convergence behaviour and even diverge for some Λ-shaped tanks. This fact can be explained by the singular behaviour of the natural modes at the contact line formed by the waterplane and the conical walls. From a mathematical point of view, if the smooth bases would be augmented by a harmonic function, which has the specified singular behaviour, the convergence can be considerably improved. Lukovsky *et al.* (1984) gave examples of such an augmented function for two-dimensional spectral sloshing problems. Dedicated mathematical studies are needed to specify a suitable singular function for our case.

Bauer (1982) and Dokuchaev (1964) compared the numerical data presented in this paper with simplified analytical approximation, which were obtained for pure conical tanks with small semi-apex angles. Satisfactory agreement was observed only for a small angle ($\theta_0 < 15°$). This agreement is consistent with the assumptions used by Bauer (1982) who replaced the planar mean liquid surface by spheric segment.

In future work, an emphasis should be placed on the shallow water sloshing. This case requires a dedicated study, which has to be based on a nonlinear dissipative sloshing model. Further, a special analysis is needed for approximate natural modes, which enable handling singular behaviour at contact line formed by the mean free surface and the rigid walls. Accounting for this singularity should improve convergence.

Nonlinear phenomena are also of importance for resonant sloshing. Results of the present paper may be utilised to improve the multimodal technique (Lukovsky, 1990; Faltinsen *et al.*, 2000; Gavrilyuk *et al.*, 2005) and to study the nonlinear sloshing in a truncated conical tank. This will be the main purpose of our forthcoming studies.

Table III.
κ_{11} versus $\theta_0$and r_1 for V-shaped tanks

$r_1 \backslash \theta_0$	10°	15°	20°	25°	30°	35°	40°	45°	50°	55°	60°	65°	70°
0.15	1.6743	1.5862	1.4950	1.4011	1.30444	1.2052	1.1037	1.0000	0.8943	0.7868	0.6777	0.5671	0.4553
0.10	1.6743	1.5862	1.4950	1.4011	1.3044	1.2052	1.1037	1.0000	0.8943	0.7868	0.6776	0.5670	0.4551
0.15	1.6743	1.5862	1.4950	1.4011	1.3044	1.2052	1.1037	1.0000	0.8941	0.7865	0.6772	0.5665	0.4547
0.20	1.6743	1.5862	1.4950	1.4011	1.3044	1.2051	1.1035	0.9996	0.8935	0.7857	0.6763	0.5655	0.4536
0.25	1.6743	1.5862	1.4950	1.4010	1.3043	1.2059	1.1030	0.9986	0.8922	0.7840	0.6742	0.5634	0.4517
0.30	1.6743	1.5862	1.4950	1.4010	1.3041	1.2043	1.1017	0.9966	0.8894	0.7806	0.6706	0.5598	0.4484
0.35	1.6743	1.5862	1.4950	1.4008	1.3034	1.2027	1.0990	0.9927	0.8845	0.7750	0.6647	0.5541	0.4433
0.40	1.6743	1.5862	1.4949	1.4002	1.3017	1.1994	1.0938	0.9857	0.8762	0.7660	0.6556	0.5456	0.4359
0.45	1.6743	1.5862	1.4945	1.3987	1.2980	1.1930	1.0846	0.9743	0.8633	0.7525	0.6425	0.5335	0.4256
0.50	1.6743	1.5860	1.4935	1.3952	1.2908	1.1816	1.0696	0.9566	0.8442	0.7332	0.6242	0.5171	0.4117
0.55	1.6743	1.5856	1.4908	1.3877	1.2774	1.1625	1.0461	0.9304	0.8171	0.7067	0.5996	0.4954	0.3936
0.60	1.6743	1.5842	1.4842	1.3730	1.2540	1.1320	1.0110	0.8932	0.7800	0.6715	0.5676	0.4676	0.3707
0.65	1.6740	1.5799	1.4697	1.3456	1.2153	1.0856	0.9607	0.8423	0.7309	0.6261	0.5271	0.4330	0.3425
0.70	1.6727	1.5683	1.4395	1.2973	1.1544	1.0181	0.8915	0.7751	0.6681	0.5693	0.4775	0.3910	0.3086
0.75	1.6674	1.5391	1.3808	1.2172	1.0632	0.9242	0.8002	0.6897	0.5905	0.5007	0.4183	0.3417	0.2691
0.80	1.6472	1.4709	1.2741	1.0918	0.9339	0.7994	0.6844	0.5850	0.4978	0.4202	0.3499	0.2851	0.2241
0.85	1.5781	1.3251	1.0945	0.9084	0.7606	0.6416	0.5438	0.4614	0.3906	0.3284	0.2727	0.2218	0.1741
0.90	1.3702	1.0471	0.8199	0.6599	0.5423	0.4521	0.3800	0.3207	0.2704	0.2267	0.1879	0.1526	0.1197
0.95	0.8631	0.5955	0.4461	0.3511	0.2849	0.2356	0.1970	0.1657	0.1394	0.1167	0.0966	0.0784	0.0615

References

Bauer, H.F. (1982), "Sloshing in conical tanks", *Acta Mechanica*, Vol. 43 Nos 3-4, pp. 185-200.

Bauer, H.F. and Eidel, W. (1988), "Non-linear liquid motion in conical container", *Acta Mechanica*, Vol. 73 Nos 1-4, pp. 11-31.

Damatty, ElA.A. and Sweedan, A.M.I. (2006), "Equivalent mechanical analog for dynamic analysis of pure conical tanks", *Thin-Walled Structures*, Vol. 44, pp. 429-40.

Damatty, El.A., Korol, R.M. and Tang, L.M. (2000), "Analytical and experimental investigation of the dynamic response of liquid-filled conical tanks", Paper No 966, Topic No 7, *Proceedings of the World Conference of Earthquake Engineering, New Zeland*, pp. 1-8.

Dokuchaev, L.V. (1964), "On the solution of a boundary value problem on the sloshing of a liquid in conical cavities", *Applied Mathematics and Mechanics (PMM)*, Vol. 28, pp. 151-4.

Dokuchaev, L.V. and Lukovsky, L.A. (1968), "The methods of determining of hydrodynamic characteristic of moving container with a partition. Izvestia A SSSR", *Mechanics of Liquid and Gas*, No. 6, pp. 205-13 (in Russian).

Dutta, S. and Laha, M.K. (2000), "Analysis of the small amplitude sloshing of a liquid in a rigid container of arbitrary shape using a low-order boundary element method", *International Journal for Numerical Methods in Engineering*, Vol. 47 No. 9, pp. 1633-48.

Dutta, S., Mandal, A. and Dutta, S.C. (2004), "Soilstructure interaction in dynamic behaviour of elevated tanks with alternate frame staging configurations", *Journal of Sound and Vibration*, Vol. 277, pp. 825-53.

Eurocode 8 (1998), "Design provisions of earthquake resistance of structures, Brussels: silos, tanks and pipelines", *European Committee for Standardisation (CEN). Eurocode 8*, Part 4.

Faltinsen, O.M., Rognebakke, O.F. and Timokha, A.N. (2003), "Resonant three-dimensional nonlinear sloshing in a square base basin", *Journal of Fluid Mechanics*, Vol. 487, pp. 1-42.

Faltinsen, O.M., Rognebakke, O.F., Lukovsky, L.A. and Timokha, A.N. (2000), "Multidimensional modal analysis of nonlinear sloshing in a rectangular tank with finite water depth", *Journal of Fluid Mechanics*, Vol. 407, pp. 201-34.

Feschenko, S.F., Lukovsky, L.A., Rabinovich, B.I. and Dokuchaev, L.V. (1969), *The Methods for Determining the Added Fluid Masses in Mobile Cavities*, Naukova Dumka, Kiev (in Russian).

Gavrilyuk, I., Lukovsky, I. and Timokha, A. (2005), "Linear and nonlinear sloshing in a circular conical tank", *Fluid Dynamics Research*, Vol. 37, pp. 399-429.

Gavrilyuk, I., Lukovsky, I., Makarov, V. and Timokha, A. (2006), *Evolutional Problems of the Contained Fluid*, Publishing House of the Institute of Mathematics of NASU, Kiev.

Ibrahim, R. (2005), *Liquid Sloshing Dynamics*, Cambridge University Press, Cambridge.

Levin, O. (1963), "Oscillation of a fluid in rectilinear conical container", *AIAA Journal*, Vol. 2 No. 6, pp. 1447-8.

Lukovsky, I.A. and Bilyk, A.N. (1985), "Forced nonlinear oscillation of a liquid in a moving axial symmetric conical tanks", in Lukovsky, I. (Ed.), *Numericalanalytical Methods of Studying the Dynamics and Stability of Multidimensional Systems*, Institute of Mathematics, Kiev, pp. 12-26 (in Russian).

Lukovsky, L.A. (1975), *Nonlinear Oscillation of a Fluid in Tanks of Complex Shape*, Naukova Dumka, Kiev (in Russian).

Lukovsky, L.A. (1984), *Approximate Methods of Solving the Problems of Dynamics of a Limited Liquid Volume*, Naukova Dumka, Kiev (in Russian).

Lukovsky, L.A. (1990), *Introduction to Nonlinear Dynamics of a Solid Body with a Cavity Filed by a Liquid*, Naukova Dumka, Kiev (in Russian).

Lukovsky, L.A. (2004), "Variational methods of solving dynamic problems for fluid-containing bodies", *International Applied Mechanics*, Vol. 40 No. 10, pp. 1092-128.

Lukovsky, L.A. and Timokha, A.N. (2002), "Modal modeling of nonlinear fluid sloshing in tanks with non-vertical walls. Non-conformal mapping technique", *International Journal of Fluid Mechanics Research*, Vol. 29 No. 2, pp. 216-42.

Mikishev, G.N. and Dorozhkin, N.Y. (1961), "An experimental investigation of free oscillations of a liquid in containers", *Izvestiya Akademii Nauk SSSR*, Mekhanika, Mashinostroenie, Otdelenie Tekhnicheskikh Nauk, No 4, pp. 48-53 (in Russian).

Mikishev, G.N. and Rabinovich, B.I. (1968), *Dynamic of the Rigid Body with a Vacuity, Partially Filled with Liquid*, Mashinostroenie, Moscow (in Russian).

Morand, J.P. and Ohayon, R. (1995), "Fluid structure interaction", *Applied Numerical Methods*, Wiley, New York, NY.

Shrimali, M.K. and Jangid, R.S. (2003), "Earthquake response of isolated elevated liquid storage steel tanks", *Journal of Constructional Steel Researchl*, Vol. 59, pp. 1267-88.

Tang, L.M. (1999), "Dynamic Behavior of Liquid-filled Circular and Conical tanks", master thesis, McMaster University, Hamilton.

Appendix

(The Appendix Figure follows overleaf.)

$\theta_0 = \pi/6$				
n	ν_{0n}	ν_{1n}	ν_{2n}	ν_{3n}
1	6.83539808	3.11959709	5.49282500	7.75244235
2	12.90828411	9.71206871	12.37204261	14.91804177
3	18.93644560	15.82152796	18.58301633	21.24614849
4	24.95138112	21.87016680	24.68578005	27.41663567
5	30.96063428	27.89785663	30.74738346	33.52289135
6	36.96692917	33.91577437	36.78860888	39.59590680
7	42.97148871	39.92832912	42.81818932	45.64932001
8	48.97494349	45.93761963	48.84047013	51.69015118
9	54.97765160	51.94477437	54.85786626	57.72240544
10	60.97983147	57.95045476	60.87183012	63.74854246
11	66.98162391	63.95507442	66.88328881	69.77015940
12	72.98312378	69.95890533	72.89286242	75.78833988
$\theta_0 = \pi/4$				
1	4.40532918	2.00000000	3.63323872	5.20142706
2	8.44711262	6.33388964	8.13729380	9.87466847
3	12.46332875	10.39698483	12.25919783	14.06452673
4	16.47193967	14.42505010	16.31855929	18.16308293
5	20.47727740	18.44103192	20.35413803	22.22447977
6	24.48090964	22.45137475	24.37794511	26.26665923
7	28.48354098	26.45862229	28.39502631	30.29751029
8	32.48553497	30.46398566	32.40789182	34.32109176
9	36.48709810	34.46811614	36.41793652	38.33971851
10	40.48835640	38.47139553	40.42599923	42.35481185
11	44.48939109	42.47406256	44.43261536	46.36729454
12	48.49025692	46.47627426	48.43814300	50.37779256
$\theta_0 = \pi/3$				
1	3.19569115	1.46798738	2.75258821	4.00000000
2	6.21952915	4.65418866	6.04042231	7.38840139
3	9.22884937	7.69054134	9.11091186	10.49837828
4	12.23380906	10.70673365	12.14521751	13.55538637
5	15.23688626	13.71595755	15.16577182	16.59087636
6	18.23898124	16.72192772	18.17952282	19.61524899
7	21.24049935	19.72611149	21.18938780	22.63307179
8	24.24164994	22.72920771	24.19681751	25.64669297
9	27.24255203	25.73159226	27.20261792	28.65745115
10	30.24327826	28.73348550	30.20727365	31.66616793
11	33.24387547	31.73502524	33.21109395	34.67337662
12	36.24437524	34.73630210	36.21428568	37.67943893

Figure A1.
Values of ν_{mn} versus θ_0

Corresponding author
A. Timokha can be contacted at: alexander.timokha@ntnu.no